Journal of Alloys and Compounds 509 (2011) 1115–1118

Contents lists available at ScienceDirect

Journal of Alloys and Compounds

journal homepage: www.elsevier.com/locate/jallcom

Ultraviolet and violet upconversion luminescence in Ho^{3+}-doped Y_2O_3 ceramic induced by 532-nm CW laser

Feng Qin [a], Yangdong Zheng [a], Ying Yu [a], Zhemin Cheng [a], Pouran Sadat Tayebi [a], Wenwu Cao [a,b], Zhiguo Zhang [a,*]

[a] Department of Physics, Harbin Institute of Technology, Harbin 150001, People's Republic of China
[b] Materials Research Institute, The Pennsylvania State University, University Park, PA 16802, United States

ARTICLE INFO

Article history:
Received 5 July 2010
Received in revised form
27 September 2010
Accepted 28 September 2010
Available online 8 October 2010

Keywords:
Holmium
Upconversion
Ultraviolet

ABSTRACT

Ultraviolet and violet upconversion luminescence spectra of holmium-doped Y_2O_3 were produced under the excitation of a compact continues-wave 532 nm solid-state laser. Emissions around 306, 362, 412, 390 and 428 nm can be assigned to the transitions of $^3D_3 \rightarrow {}^5I_J$ ($J = 8, 7, 6$), $^5G_4 \rightarrow {}^5I_8$ and $^5G_5 \rightarrow {}^5I_8$, respectively. Power dependence and upconversion dynamics analysis demonstrated that both the energy transfer upconversion (ETU) and the excited state absorption (ESA) processes were involved in the population of $^3D_3$ state via the coupled intermediate states $^5S_2/{}^5F_4$. Fluorescence spectra in the visible and infrared ranges showed that $^5G_4$ and $^5G_5$ states were populated by the ESA process from $^5I_6$ and $^5I_7$ states, respectively, while the $^5I_6$ and $^5I_7$ states were radiatively populated from the excited $^5S_2/{}^5F_4$ states. Upconversion mechanisms have been evaluated based on a rate equation model.

1. Introduction

Potential applications in environmental sciences, medicine, photolithography, material processing, and high-density optical data storage have stimulated the development of solid-state lasers working in the ultraviolet (UV) spectral range [1,2]. Frequency upconversion (UC) is one method to produce short wavelength laser, pumped with relatively longer wavelength laser through intrinsic energy level matching of certain rare-earth ions [3]. In UC process, high-lying excited states whose energy exceeds that of the pump photon are populated by multi-photon interaction processes such as excited state absorption (ESA), energy transfer upconversion (ETU) and photon avalanche (PA) [4].

Recently, generation of upconverted fluorescence by infrared (IR) lasers has attracted great interest due to the availability of inexpensive commercial IR diode lasers. However, in order to induce a single UV photon the active ion has to absorb at least three IR photons or even more [5]. Usually, with the increase of photons involved in an upconversion process, the upconversion mechanism becomes more complex and the upconversion efficiency goes down. Therefore, compared with shorter wavelength lasers, low cost IR diode laser is less efficient to induce UV upconversion emissions.

Traditional visible lasers, such as argon-krypton lasers, are expensive, bulky and complex in structure. These shortcomings greatly restrict the development of such lasers for practical applications. In recent years, the development of commercial solid state Nd^{3+} lasers has made significant progress. High-power and cost-effective compact 532-nm continuous wave (CW) solid state laser is now readily available. More importantly, the energy of such green laser matches well with the energy structures of trivalent holmium ions so that the green laser can resonate with the thermalized $^5S_2/{}^5F_4$ states [6].

Trivalent holmium ion (Ho^{3+}) itself is a good candidate for upconversion processes because it has many long-lived intermediate metastable levels, from which excited state absorption (ESA) can take place [7,8]. There are also several high-lying metastable levels that can give rise to transitions at various wavelengths in the visible and UV regions [9]. Most upconversion studies on Ho^{3+}-doped materials were mainly focused on infrared and visible regions. There are also a few papers devoted to the studies of UV and violet upconversion fluorescence under IR or red laser excitation [5,7,10,11]. Here we report the generation of blue, violet, and ultraviolet upconversion luminescence spectra in the range of 290–450 nm by the excitation of a compact continues-wave 532 nm green solid-state laser in Y_2O_3:Ho^{3+} ceramic. The corresponding upconversion mechanisms are analyzed by means of power dependence and temporal evolution curves of upconverted fluorescence spectra in visible and infrared ranges. The proposed upconversion mechanisms are evaluated using proper rate equations.

* Corresponding author.
E-mail address: zhangzhiguo@hit.edu.cn (Z. Zhang).

0925-8388/$ – see front matter © 2010 Elsevier B.V. All rights reserved.
doi:10.1016/j.jallcom.2010.09.188

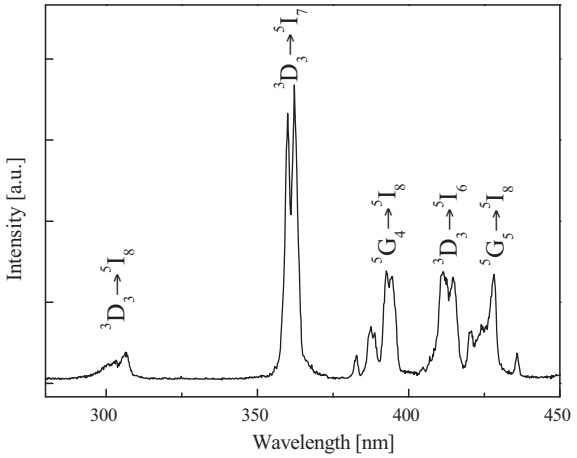

Fig. 1. Upconversion emission spectrum of Y_2O_3:Ho^{3+} under 532-nm laser excitation.

2. Experimental procedure

Yttrium (III) oxide (Y_2O_3) powders doped with Ho^{3+} 1 mol% were prepared by the following complex precursor method. $Y(NO_3)_3$ and $Ho(NO_3)_3{\cdot}6H_2O$ with proportional molar ratios of cations were completely dissolved in de-ionized water by constant rate stirring at 80 °C. Subsequently, citric acid was added into the solution with 1:4 molar ratio of (Y + Ho) to citric acid. After complete dissolution, the pH of the solution was adjusted to 6.0 by the addition of ammonium hydroxide. The resulting solution was dried at 180 °C for 24 h and then transformed into a black bulk. This black bulk was calcined at 900 °C for 2 h in air to remove remained organic additives so that the nanocrystals were formed. These nanocrystals were pressed under 10 MPa pressure into a smooth and flat disk, then sintered at 1300 °C for 32 h in air to form ceramic samples.

X-ray diffraction showed that the sample is in pure phase with cubic crystal structure. The ceramic sample was excited by a 532-nm laser (CLO Laser DPGL-500L), and the resulting emissions were analyzed using a medium resolution monochromator (Zolix SBP300). Florescence in the UV and visible ranges was detected by a photomultiplier tube (Zolix CR131) and in IR range by a PbS detector (Zolix DPbS2900). These detected signals were amplified and plotted on a chart recorder (Zolix DSC102). To measure the fluorescence lifetime, the CW laser was modulated by an electro-optic modulator (Leysop EM200K) with square wave modulation and the induced time-resolved curves were recorded by a digital phosphor oscilloscope (Tektronix TDS 5052).

3. Results and discussions

Fig. 1 is the upconverted emission spectrum of Y_2O_3:Ho^{3+} ceramic in the range of 290–450 nm under the excitation of a 532 nm green light laser. Five emission bands centered at 306, 362, 390, 412 and 428 nm were generated by intra-4*f* electron transitions of Ho^{3+} ions. Emissions around 306, 362, and 412 nm can be assigned to the transitions from $^3D_3$ state to the ground state $^5I_8$ and the first two excited states $^5I_7$ and $^5I_6$, respectively, corresponding well to the fluorescence emissions excited by the 288 nm pumping light [9]. Peaks centered at 390 and 428 nm can be assigned to the transitions $^5G_4 \rightarrow {}^5I_8$ and $^5G_5 \rightarrow {}^5I_8$ of the Ho^{3+} ions [5]. The energy level diagram of the Ho^{3+} ion and corresponding transitions are indicated in Fig. 2 [12].

The upconversion mechanisms for trivalent holmium ion pumped by the 532-nm laser are proposed as illustrated in Fig. 2. Ho^{3+} ions in the ground state are pumped to the thermalized $^5S_2/^5F_4$ states by ground state absorption (GSA) process. Subsequently the $^3D_3$ state is populated by way of either ETU or ESA process utilizing the $^5S_2/^5F_4$ states as the intermediate level, which then produces 306, 362, and 412-nm luminescence. The $^5G_4$ and $^5G_5$ states are populated by ESA processes from the $^5I_6$ and $^5I_7$ states resulting in the 390 and 428-nm emissions, respectively.

In order to identify the ESA processes from low excited states, the population situation of these states needs to be investigated. For this purpose, the fluorescence spectra under the single green

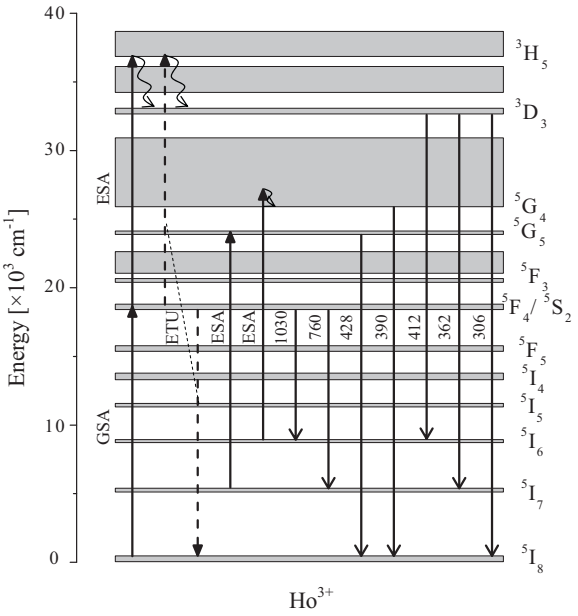

Fig. 2. Partial energy-level diagrams of Ho^{3+} ions and proposed upconversion emission mechanism.

laser irradiation are measured. Fig. 3 is the recorded spectrum in the visible range. Emissions peaked at 550 and 760 nm can be assigned to transitions from the thermalized levels $^5S_2/^5F_4$ to the ground state $^5I_8$ and the first excited state $^5I_7$, respectively. The relatively weaker luminescence around 660 nm in the inset of Fig. 3 corresponds to the $^5F_5 \rightarrow {}^5I_8$ transition. As illustrated in Fig. 3, the emission from $^5F_5$ level (660 nm) is so weak compared with the $^5S_2/^5F_4 \rightarrow {}^5I_7$ transition (760 nm) that the population of such level could be neglected. That is to say, the probability of normally radiationless relaxation from the $^5S_2/^5F_4$ states to $^5F_5$ state is greatly decreased due to the resonating nature of the pumping green light with the coupled $^5S_2/^5F_4$ states in the Y_2O_3 ceramic. Additionally, the significant luminescence around 760 nm indicates that the $^5I_7$ state could be directly populated by the thermalized $^5S_2/^5F_4$ levels radiatively under the green laser excitation rather than nonradiative relaxation from the $^5F_5$ state [13].

Fig. 4 shows the IR fluorescence spectrum. There are three emission bands centered at 1.03, 1.2 and 2.0 μm. The 1.03 μm emission corresponds to the $^5S_2/^5F_4 \rightarrow {}^5I_6$ transition, while luminescence around 1.2 and 2.0 μm can be assigned to transitions from $^5I_6$

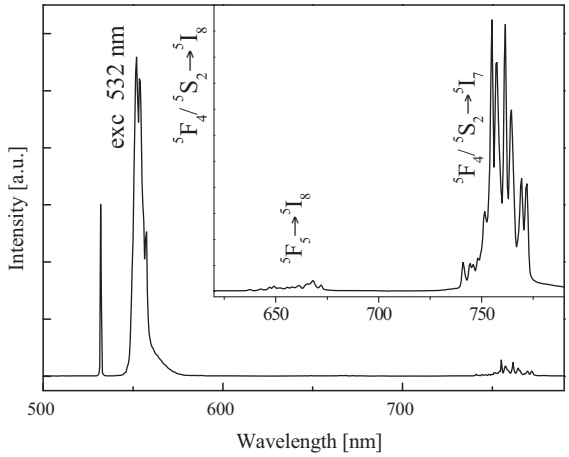

Fig. 3. Visible emission spectrum of Y_2O_3:Ho^{3+} following the 532 nm laser excitation.

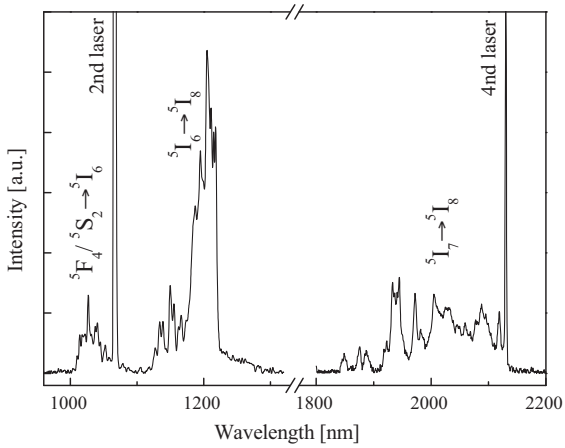

Fig. 4. Infrared emission spectrum of Y_2O_3:Ho^{3+} following the 532 nm laser excitation.

and $^5I_7$ levels to the ground state $^5I_8$, respectively. That is to say, both $^5I_6$ and $^5I_7$ states are populated from the excited thermalized level ($^5S_2/^5F_4$) radiatively. Therefore, considering the long-lived metastable states $^5I_6$ and $^5I_7$, it is reasonable to propose that $^5G_4$ and $^5G_5$ states are populated by ESA processes from $^5I_6$ and $^5I_7$ states, respectively.

To identify which multi-photon process is responsible for these upconversion emissions, the emission intensities were measured as a function of the pumping power. For an unsaturated upconversion process, the upconverted emission intensity (I_{em}) depends on the pumping laser power (I_{pump}) according to the following relation:

$$I_{em} \propto I_{pump}^{n}, \quad n = 2, 3, \ldots \tag{1}$$

where n is the number of pumping photons absorbed per short wavelength photon emitted, which can be easily evaluated from the slope of the linear fit. Fig. 5 shows the logarithmic plot of the integrated emission intensities of the upconverted emissions. As illustrated in Fig. 5, the n values are 2.1, 2.0 and 2.0 for the 306, 362, and 412-nm emission bands, respectively. Therefore, two-photon process was involved in populating the emitting state. Moreover, the same n value of the three emission peaks provides further evidence that these emissions all originate from the same state. However, the n values for the 390 and 428-nm peaks are only 1.5 and 1.2, respectively. Although the n values also suggest that $^5G_4$ and $^5G_5$ states are both populated by two-photon process, the relatively smaller n indicates that the populating manners for these two states are different.

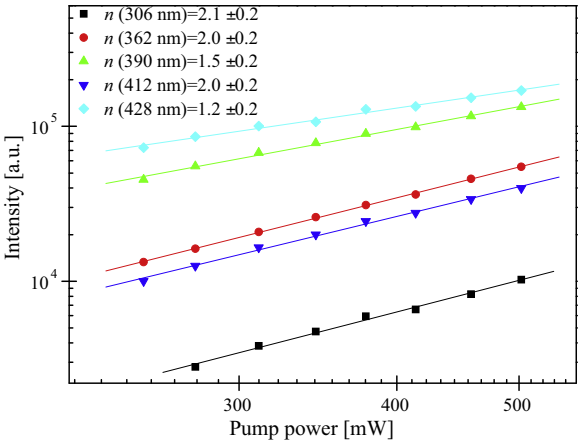

Fig. 5. Logarithmic plot of the observed upconversion emission intensities versus pumping laser power.

In order to describe the above mentioned processes, differential equations of states are proposed as following:

$$\frac{dn_1}{dt} = n_3A_{31} - n_1A_1 - \sigma_{14}\rho n_1, \tag{2a}$$

$$\frac{dn_2}{dt} = n_3A_{32} - n_2A_2 - \sigma_{25}\rho n_2, \tag{2b}$$

$$\frac{dn_3}{dt} = \sigma_{03}\rho n_0 - n_3A_{30} - n_3A_{31} - n_3A_{32}, \tag{2c}$$

$$\frac{dn_4}{dt} = \sigma_{14}\rho n_1 - n_4A_4, \tag{2d}$$

$$\frac{dn_5}{dt} = \sigma_{25}\rho n_2 - n_5A_5, \tag{2e}$$

where n_0, n_1, n_2, n_3, n_4, and n_5 are the population of the $^5I_8$, $^5I_7$, $^5I_6$, $^5S_2/^5F_4$, $^5G_5$ and $^5G_4$ levels, respectively, σ_{ik} is the absorption across section between the i and k states, ρ is the pumping energy density, and A_{ik} is the radiative transition probability. Here we assume that linear decay dominates the $^5S_2/^5F_4$ states, therefore, the upconversion term in Eq. (2c) is negligible. For the $^5G_5$ state, under the steady-state excitation, we have

$$n_4A_4 = \frac{n_0\sigma_{03}\sigma_{14}A_{31}}{A_{30}+A_{31}+A_{32}}\frac{\rho^2}{A_1+\sigma_{14}\rho}. \tag{3}$$

When $A_1 \gg \sigma_{14}\rho$, that is to say, the main depletion mechanism for $^5I_7$ state is a linear decay, $n_4A_4 \propto \rho^2$. When $A_1 \ll \sigma_{14}\rho$, which means upconversion is dominant for $^5I_7$ state, $n_4A_4 \propto \rho$. Therefore, for the $^5I_7$ state, upconversion is a dominant depletion mechanism compared with the linear decay [14]. Similarly, for the $^5G_4$ state, we have

$$n_5A_5 = \frac{n_0\sigma_{03}\sigma_{25}A_{32}}{A_{30}+A_{31}+A_{32}}\frac{\rho^2}{A_2+\sigma_{25}\rho}. \tag{4}$$

According to the above discussion, for the $^5I_6$ state, upconversion is a depletion mechanism comparable with linear decay [14]. Such explanation is reasonable considering the long lifetimes of the $^5I_7$ and $^5I_6$ states which are in the order of tens of milliseconds [13].

There are two possible approaches to populate the $^3D_3$ state, i.e., either ETU or ESA process utilizing the intermediate $^5S_2/^5F_4$ states. To identify which one is the actual physical mechanism, fluorescence decays from concerned levels were measured. Typical decay curves are plotted in Fig. 6 in logarithmic scale. For the $^3D_3$ state, the decay curves have been fitted to two-exponential decay law and the estimated decay times are obtained: $\tau_1 = 15 \pm 2$, $\tau_2 = 57 \pm 3$ μs for the 362 nm emission and $\tau_1 = 15 \pm 2$, $\tau_2 = 58 \pm 3$ μs for the 414 nm emission. Such results indicate that an energy transfer upconversion process is involved in populating the $^3D_3$ level although the excited state absorption process cannot be ruled out. Decay curves for the emissions from $^5S_2/^5F_4$ states are fitted to single-exponential decay law and the decay times are fitted to be 113 ± 3 and 115 ± 3 μs for the 550 and 760 nm emissions, respectively. These results confirmed that the luminescence peaked at 550 and 760 nm originate from the same excited state.

In order to describe the physical mechanism of the $^3D_3$ state, differential equations of corresponding states are proposed as follow:

$$\frac{dn_3}{dt} = \sigma_{03}\rho n_0 - A_3n_3, \tag{5a}$$

$$\frac{dn_D}{dt} = \sigma_{3D}\rho n_3 + W{n_3}^2 - A_Dn_D, \tag{5b}$$

where n_D is the population of the $^3D_3$ level, σ_{ik} is the absorption across section between the i and k states, ρ is the pumping energy density, W is the corresponding parameter of ETU process, and A_i

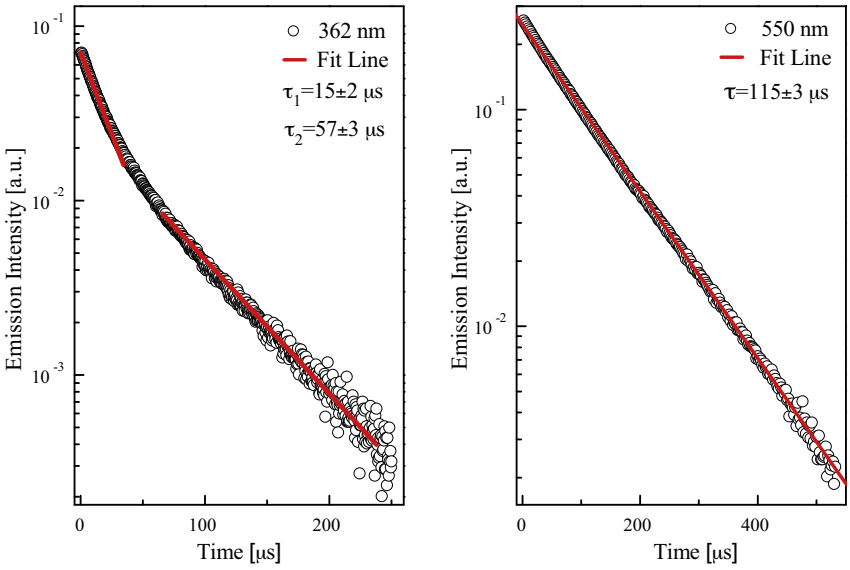

Fig. 6. Typical temporal evolution of the $^3D_3$ and $^5S_2/^5F_4$ states after 532 nm excitation.

is the radiative transition probability. We neglected the upconversion decay term for $^5S_2/^5F_4$ states. Under steady-state excitation, stationary solutions are deduced so that

$$n_{30} = \frac{\sigma_{03}\rho n_0}{A_3}, \tag{6a}$$

$$n_{D0} = \frac{\sigma_{03}\rho^2 n_0}{A_D A_3}\left(\sigma_{3D} + \frac{W\sigma_{03}n_0}{A_3}\right). \tag{6b}$$

For decay processes, there are no pump terms in the above equations, thus we could get the following solutions from Eq. (5):

$$n_3 = n_{30}\exp(-A_3 t), \tag{7a}$$

$$n_D = C_1\exp(-A_D t) + C_2\exp(-2A_3 t), \tag{7b}$$

with the initial conditions $n_3(t=0)=n_{30}$ and $n_D(t=0)=n_{D0}$. Here the integral parameters are calculated to be $C_1=(\sigma_{01}\rho^2 n_0/A_3A_D)(\sigma_{12}-(2W\sigma_{01}n_0/(A_D-2A_3)))$ and $C_2=(W\sigma_{01}^2\rho^2 n_0^2/A_3^2(A_D-2A_3))$, respectively.

According to above analyses, the two-exponential decay curves of $^3D_3$ state can be interpreted as follows: the fast decay (τ_1) corresponds to the radiative lifetime of $^3D_3$ state, i.e., $\tau_{D1}=1/A_D=\tau_D$; the slow decay (τ_2) is caused by the energy transfer upconversion process from the pumped thermalized levels $^5S_2/^5F_4$, whose decay time is twice of the slow decay time (τ_2), i.e., $\tau_{D2}=1/2A_3=\tau_3/2$. This means that the $^3D_3$ state could be populated by the ETU process. However, the ESA process cannot be ruled out because the signs of C_1 and C_2 are both positive. If there is no ESA process, the σ_{12} term will not exist so that the sign of C_1 should be opposite to that of C_2, and this does not agree with our experiment results.

Based on the arguments above, we propose the following upconversion mechanisms for trivalent holmium ion pumped by a 532-nm laser: Ho^{3+} ion in the ground state is pumped to the $^5S_2/^5F_4$ states by the GSA process. Then, the excited $^5S_2/^5F_4$ states populate the $^5I_6$ and $^5I_7$ states radiatively, and subsequently, the ESA processes take place from these two levels, resulting in the population of the $^5G_4$ and $^5G_5$ states, which are responsible for the 390 and 428-nm emissions, respectively. Meanwhile, the $^3D_3$ state of Ho^{3+} ion, which is responsible for the 306, 362, and 412-nm luminescence, is populated by both the ETU and ESA processes, using the thermalized $^5S_2/^5F_4$ states as the intermediate state.

4. Conclusion

In this paper, we report the observation of ultraviolet and violet upconversion luminescence in Y_2O_3:Ho^{3+} (1 mol%) ceramic under the excitation of a 532 nm CW green laser. The emissions peaked at 390 and 428 nm are originated from the $^5G_4$ and $^5G_5$ states, which are populated by ESA processes from two long-lived low excited states. This process is identified experimentally by power dependent curves and explained by a steady state rate equation model. The luminescence spectra around 306, 362, and 412 nm are originated from the $^3D_3$ state, which is populated by both the ETU and ESA processes. Such populating approaches are identified based on fluorescence decay curves and analyzed by a time dependent rate equation model.

Acknowledgment

This work was financially supported by the 863 Hi-Tech Research and Development Program of the People's Republic of China.

References

[1] X. Zhang, C. Serrano, E. Daran, F. Lahoz, G. Lacoste, A. Muñoz-Yagüe, Phys. Rev. B 62 (2000) 4446.
[2] C.L. Pope, B.R. Reddy, S.K. Nash-Stevenson, Opt. Lett. 22 (1997) 295.
[3] L.F. Johnson, H.J. Guggenheim, Appl. Phys. Lett. 19 (1971) 44.
[4] M.-F. Joubert, Opt. Mater. 11 (1999) 181.
[5] X.X. Luo, W.H. Cao, Mater. Lett. 61 (2007) 3696.
[6] K.L. Nash, R.C. Dennis, N.J. Ray, J.B. Gruber, D.K. Sardar, J. Appl. Phys. 106 (2009).
[7] F. Lahoz, I.R. Martin, J.M. Calvilla-Quintero, Appl. Phys. Lett. 86 (2005).
[8] M. Malinowski, A. Wnuk, Z. Frukacz, G. Chadeyron, R. Mahiou, S. Guy, M.F. Joubert, J. Alloys Compd. 323 (2001) 731.
[9] M. Malinowski, M. Kaczkan, A. Wnuk, M. Szuflinska, J. Lumin. 106 (2004) 269.
[10] D.Y. Wang, Y. Min, W.P. Zhang, D. Ning, Y.S. Zhang, S.D. Xia, J. Alloys Compd. 361 (2003) 1.
[11] M. Kaczkan, M. Malinowski, J. Alloys Compd. 380 (2004) 201.
[12] M. Malinowski, R. Piramidowicz, Z. Frukacz, G. Chadeyron, R. Mahiou, M.-F. Joubert, Opt. Mater. 12 (1999) 409.
[13] M. Malinowski, Z. Frukacz, M. Szuflinska, A. Wnuk, M. Kaczkan, J. Alloys Compd. 300 (2000) 389.
[14] M. Pollnau, D.R. Gamelin, S.R. Lüthi, H.U. Güdel, Phys. Rev. B 61 (2000) 3337.